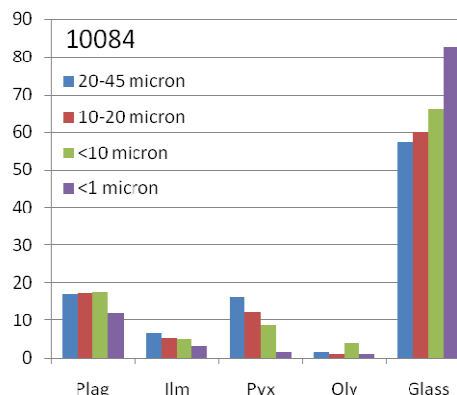


**THE SMALLEST LUNAR GRAINS: ANALYTICAL TEM CHARACTERIZATION OF THE SUB-MICRON SIZE FRACTION OF A MARE SOIL.** M. Thompson<sup>1</sup> and R. Christoffersen<sup>2</sup>, <sup>1</sup>Department of Geological Sciences and Engineering, Queen's University, Kingston, ON, Canada, K7L3N6, 5mt26@queensu.ca, <sup>2</sup>Jacobs Technology, ESCG, Mail Code JE23, Houston, TX, 77058, roy.christoffersen-1@nasa.gov.

**Introduction.** The chemical composition, mineralogical type, and morphology of lunar regolith grains changes considerably with decreasing size [1,2,3], and below the ~25  $\mu\text{m}$  size range the correlation between these parameters and remotely-sensed lunar surface properties connected to space weathering increases significantly [1,2]. Although trends for these parameters across grain size intervals greater than 20  $\mu\text{m}$  are now well established [1,2,3], the 0 to 20  $\mu\text{m}$  size interval remains relatively un-subdivided with respect to variations in grain modal composition, chemistry and microstructure. Of particular interest in this size range are grains in the approximate < 1  $\mu\text{m}$  diameter class, whose fundamental properties are now the focus of lunar research pertaining to electrostatic grain transport [4,5], dusty plasmas [5], and lunar dust effects on crew health and exploration systems [6]. In this study we have used analytical transmission electron microscopy (TEM) to characterize the mineralogy, microstructure and major element composition of grains below the 1  $\mu\text{m}$  size threshold in lunar soil 10084.

**Samples and Methods:** Lunar regolith sample 10084 is a representative mature mare soil ( $I_s/\text{FeO} = 78$  [3]) that prior studies have shown contains some evidence of mixing with highland material [2,3]. Settling experiments were performed in ethanol using <20  $\mu\text{m}$  sieved material in order to concentrate grains of this size fraction for TEM study. Stokes law calculations indicated this method would induce minimal biases into the grain modal compositions based on grain density. After 2 hours of gravity induced settling, a droplet was withdrawn and placed on a continuous carbon film TEM grid and evaporated. TEM observations confirmed that this method produced a high concentration of < 1  $\mu\text{m}$  grains that were adequately thin for quantifiable energy-dispersive x-ray analysis (EDX). Grains below a threshold size of 1  $\mu\text{m}$  were selected at random and subjected to digital bright-field imaging and EDX analysis with conversion of peak intensities to element concentrations using the Cliff-Lorimer method [7].

**Modal/Grain Type Composition of Sub-Micron Grains:** A total of 200 grains < 1  $\mu\text{m}$  in size were individually imaged and chemically analyzed and their overall modal composition is compared to data for 10084 large size fractions in Figure 1. A total of 80% are diverse types of glasses, representing a significant increase in this grain type relative to the 65% fraction



**Figure 1.** Modal composition (percent) of < 1  $\mu\text{m}$  grains in lunar soil 10084 compared to data for larger size fractions [3].

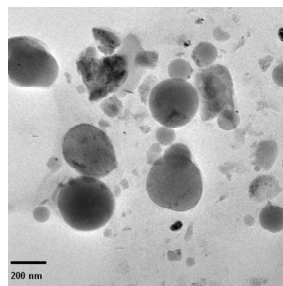


**Figure 2.** Bright-field TEM images of < 1  $\mu\text{m}$  glass spherules in lunar soil 10084.

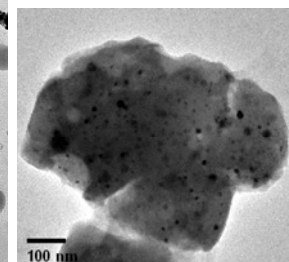


**Figure 3.** Bright-field TEM images of glass grain containing nanophase  $\text{Fe}^0$ .

Table 1. Modal composition of sub-micron mineral grains in 10084

Mineral Type	Fraction of Total %	Mineral Fraction %
Plagioclase	12.4	70.3
Ilmenite	2.9	16.2
Pyroxene	1.4	8.1
Olivine	1.0	5.4

of glass grains in the inclusive <10  $\mu\text{m}$  size fraction as a whole [3] (Fig. 1). On a morphological/microstructural basis the 80% subpopulation of sub-micron glass grains is comprised of 45% (36% of total) spherules that generally contain little or no nanophase  $\text{Fe}^0$  (Fig. 1), and roughly 45% (36% of total) oblong or irregularly shaped grains that contain various amounts of nanophase  $\text{Fe}^0$  (Fig. 2). The remaining 10% (8% of total) are hybrid types, e.g., spherules that contain significant nanophase  $\text{Fe}^0$ . Besides the wholly-glass

grains, the number of grains that could be classified as either glass-mineral or mineral-glass aggregates (i.e., “nano-agglutinates”) was surprisingly small (<2% of total sample). The bulk of the remaining population of analyzed grains therefore consisted of discrete mineral grains whose modal proportions are shown in Table 1. These have diverse shapes and microstructural aspects reflecting various space weathering processes.

**Composition and Chemical Variation Trends of Glass Grains:** The predominance of glass grains that were individually homogeneous allowed us to use single-point EDX analyses as a basis for compositional analyses similar to those used in previous studies of larger lunar soil glass grains [8,9]. These previous studies defined two broad compositional groups of glassy grains, one associated with impact-associated volatilization/vapor condensation processes and the other with impact melting. The former involves substantial chemical evolution of the grains from the original impact target, while the other retains most of the elements in the melted material that formed the grain. For grains affected by volatilization there is a predictable distribution of glass compositions with respect to volatile content; more  $\text{Al}_2\text{O}_3$  and CaO indicates greater volatile depletion, as with the HASP (High Aluminum Silica Poor) glasses, and more FeO and  $\text{SiO}_2$  is representative of higher volatile element content as in the VRAP grains (Volatile-Rich-Al-Poor) [8,9]. By plotting our glass grain compositions based on these parameters in Figure 4, we can identify compositions with HASP and VRAP affinities at the upper and lower ends of the data trend respectively (Fig. 4). The data identify approximately 28% HASP grains and 12% VRAP grains in the total glass grain population (Table 2). This significant proportion supports the notion that these grain types would be more prevalent in smaller size fractions due to the high surface area-to-volume ration necessary to promote vapor-mediated chemical changes. Additional sub-division of the HASP grain types into those with highland or mare affinity is possible based on a combination of total  $\text{FeO}+\text{MgO}+\text{TiO}_2$  contents and  $\text{CaO}/\text{Al}_2\text{O}_3$  ratios, resulting in approximately 11% highland and 6% mare affinity within the HASP group (Table 2). An additional 9% of HASP grains of indeterminate type (Table 2) based on the previous criteria were analyzed based on  $\text{Al}_2\text{O}_3$  versus  $\text{SiO}_2$  trends and found to show evidence of highland affinity, making nearly 20% of all HASP glasses in the sub-micron 10084 soil derived from highland soil. This may suggest an increase in highland-to-mare soil mixing as grains decrease into this finest size fraction [2]. The remaining compositional groups of grains in the middle of the trend in Figure 4 may be glasses largely unaffected by volatilization. One sub-population in this

group (“outliers”, Fig. 4) falls off the trend line and may be “monomineralic” melts from single mineral grains.

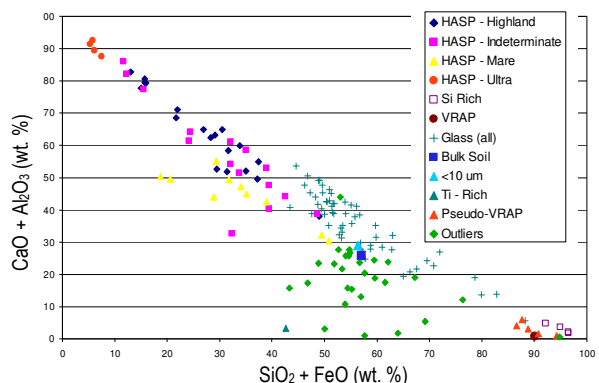


**Figure 4.** Plot of measured  $\text{CaO}+\text{Al}_2\text{O}_3$  compositions versus  $\text{SiO}_2 + \text{FeO}$  for all sub-micron 10084 soil glass grains examined in the current study.

Table 2. Sub-micron glass grain compositional types in 10084

Glass Grain Type	Fraction of Glass (%)
HASP (General)	28.0
• Ultra	• 2.3
• Mare	• 5.8
• Highland	• 11.1
• Indeterminate	• 8.7
Volatile Rich Glasses	11.6
• VRAP	• 1.2
• PVRAP <sup>¶</sup>	• 8.1
• High Si	• 2.3
Other Glass	60.4
• Agglutinate	• 13.4
• Glass and Mineral <sup>§</sup>	• 2.3
• All Other	• 44.7

**References:** [1] Taylor, L.A et al. (2001) *Met. & Planet. Sci.*, v. 36, 285-299. [2] Pieters C. M. and Taylor L. A. (2003) *GRL* 30:20, 2048, [3] Taylor L.A. et al (2001) *JGR*, 106, 27985-28000. [4] Stubbs T. J. et al. (2006) *Adv. Space Research*, 37, 59-66. [5] Horanyi M. (1996) *Ann. Rev. Astrn. and Aphys.*, 34, 383-418. [6] Tranfield E. et al. (2009) Lunar Airborne Dust Toxicity Advisory Group (LADTAG) Research Working Group (RWG). NLSI lunar science conference, abstract #2125. [7] Cliff, G. and Lorimer, G.W. (1975) *J. Microscopy*, v. 103, 203.. [8] Norris J.A., Keller L.P. and McKay D.S (1992) *Lunar Science Inst. Workshop on the Geology of the Apollo 17 Landing Site*, p. 44-45 [9] Norris J.A., Keller L.P. And McKay D.S (1993). *Lunar and Planetary Institute- 24th LPSC, Part 3*, p. 1093-1094.